PHYSICAL REVIEW B **71**, 180413(R) (2005)

Direct observation of a coupling between spin, lattice and electric dipole moment in multiferroic $YMnO_3$

Seongsu Lee,[1] A. Pirogov,[1] Jung Hoon Han,[1,2] J.-G. Park,[1,2,*] A. Hoshikawa,[3] and T. Kamiyama[3]
[1]*Department of Physics and Institute of Basic Science, SungKyunKwan University, Suwon 440-746, Korea*
[2]*Center for Strongly Correlated Materials Research, Seoul National University, Seoul 151-742, Korea*
[3]*Institute of Materials Science, KEK, Tsukuba-shi, Ibaraki 305-0801, Japan*
(Received 4 March 2005; published 27 May 2005)

$YMnO_3$ has an antiferromagnetic transition at 76 K with a ferroelectric transition at much higher temperature, making it a rare example of systems having both ferroelectric and magnetic transitions and thus a so-called multiferroic compound. Through high-resolution neutron diffraction studies, we have demonstrated here that at the antiferromagnetic transition of $YMnO_3$ there is a strong coupling between the spin and lattice degrees of freedom splitting two Mn–O(3) and Mn–O(4) bond distances on a basal plane. This coupling then induces an unmistakable change in the electric dipole moments, i.e., a coupling between the magnetic and electric dipole moments. We discuss how this rare phenomenon can occur within a Ginzburg-Landau theory.

DOI: 10.1103/PhysRevB.71.180413 PACS number(s): 75.50.Ee, 77.90.+k, 61.12.Ld

Recent discoveries that both ferroelectric and ferromagnetic/antiferromagnetic transitions can occur and coexist in several so-called multiferroic compounds have huge technological implications as well as immense scientific interest.[1] The key and ultimate goal of the studies on such materials is how to control one degree of freedom through the other. In order to achieve its potential applications envisaged so far, we ought to understand how they are coupled to one another at a microscopic level. Although there has been some experimental evidence supporting the existence of such a coupling, it still remains a largely open question how the proposed coupling between the two degrees of freedom is actually realized in a specific system.

Rare-earth manganites $R\mathrm{MnO}_3$ crystallize in two possible symmetries: orthorhombic and hexagonal phases. The orthorhombic phase with space group *Pbnm* is found for R=La, Pr, Nd, Sm, Eu, Gd, Tb, and Dy, i.e., rare-earth elements with large ionic radiis,[2] and these perovskites are well known to display colossal magnetoresistance properties upon doping.[3] On the other hand, the hexagonal phase with space group $P6_3cm$ is found for R=Ho, Er, Tm, Yb, Lu, Y, and Sc, which possess relatively small ionic radiis.[4] All hexagonal manganites are believed to exhibit both ferroelectric and antiferromagnetic transitions and so belong to the rare class of multiferroic systems.

$YMnO_3$ is one of the most intensively studied hexagonal manganites. Recent structural studies together with theoretical calculations revealed that electric polarization at high temperature is originated from the buckling of MnO_5 polyhedra accompanied by the displacements of Y ions.[5] Upon cooling below 80 K, Mn moments begin to order antiferromagnetically with moments aligned on the *ab* plane with a 120° structure. Previous neutron diffraction studies focusing on the low Q region, i.e., with a high d spacing, found that the magnetic structure of Mn moments is either Γ_1 or Γ_3 and the ordered moment at 10 K is found to be 2.9 μ_B, much smaller than the ionic value of 4 μ_B.[6,7] This reduction in the ordered moment is believed to be due to combined effects of the geometrically frustrated triangular Mn network and strong two dimensionality of the magnetic order. The spin wave of the ordered moments is consistent with theoretical calculations based on a two-dimensional (2D) Heisenberg model Hamiltonian according to recent inelastic neutron scattering experiments.[8,9]

As regards the question of a possible coupling between the ferroelectric and antiferromagnetic degrees of freedom, an early experimental indication is an anomaly found in the dielectric constant and loss tangent curve at T_N.[10] However, the most compelling evidence supporting such a coupling can be found in the spatial map of both ferroelectric and antiferromagnetic domains investigated by using optical second harmonic generation,[11] which uncovered that there is a strong coupling between the structure of the two domains of different nature. Although such findings themselves are very important in pointing out a possible coupling between the two degrees of freedom, it is fair, however, to say that it still remains largely unanswered how such a coupling occurs at a microscopic level.

Here we report our recent high-resolution neutron powder diffraction studies which reveal that at the antiferromagnetic transition temperature there are distinct changes in all seven atomic positions. Although these changes do not lower the crystal symmetry of $P6_3cm$ within the resolution of our experiments, they nevertheless split the otherwise almost equivalent two Mn-O(3) and Mn-O(4) distances on the basal plane. Based on the assumption of nominal charge valences, we could demonstrate that this structure change in fact induces further coupling between the antiferromagnetic and ferroelectric degrees of freedom.

For our experiment, we used $YMnO_3$ of 99.9% purity from Superconductive Components, Inc. Our high-resolution neutron powder diffraction experiment was carried out from 300 to 10 K using a time-of-flight diffractometer, SIRIUS, at the neutron scattering facility (KEKS) of the High Energy Accelerator Research Organization (KEK). The data were taken for approximately 2 h for each measurement. The resolution of our data is $\Delta l/l \approx 9\times10^{-4}$. Rietveld refinement was performed using the RIETAN-2001T program.[12]

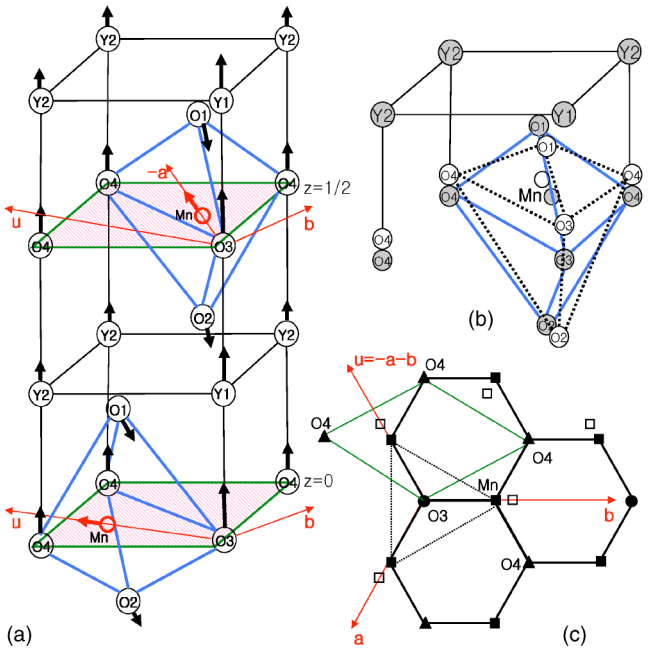

FIG. 1. (Color online) (a) Schematic representation of the crystal structure of hexagonal $YMnO_3$. The arrows indicate the displacement of each ion within the unit cell when the temperature drops below T_N. Please note that the temperature dependence of the lattice constants is not taken into account here. (b) The tilting of the MnO_5 bipyramid is shown: solid (filled symbols) and dashed (open symbols) lines represent bipyramid above and below T_N, respectively. (c) A sketch of the $z=0$ layer of $YMnO_3$, showing Mn–O bonds: Mn, O(3), and O(4) are shown as filled squares, circles, and triangles, respectively. The filled and open squares are for the Mn positions above and below T_N, respectively.

Figure 1(a) shows the schematic picture of the crystal structure of hexagonal $YMnO_3$. In the hexagonal structure, Mn atoms are located at the center of the MnO_5 bipyramids whose vertices are occupied by oxygen atoms. One O(3) and two O(4) atoms are on the equatorial plane of the MnO_5 polyhedra while O(1) and O(2) are located at apical positions. The bipyramids are linked by the corner-sharing equatorial oxygens. The arrows show the displacement of each ion when the temperature decreases below T_N. The tilting of the MnO_5 is illustrated by the dashed line in Fig. 1(b), and the movement of the in-plane Mn atom is illustrated in Fig. 1(c). According to our analysis discussed below, Y(1), Y(2), O(3), and O(4) atoms change their positions along the positive direction of the c axis with decreasing temperature while apical oxygens O(1) and O(2) move in the same direction on the ac plane below the T_N point.

Typical data taken at 10 K are shown in Fig. 2. Given that there are only weak magnetic peaks in the considerably low d range of our neutron diffraction measurements, we did not include the magnetic structure in the Rietveld refinement. For the experimental temperature range, we did not observe any peak splitting or additional peak in the neutron diffraction patterns. This indicates that the structure remains in the space group ($P6_3cm$) over the whole temperature range. Using RIETAN-2001T, we analyzed the data with reasonable agreement factors: for example, agreement factors of final

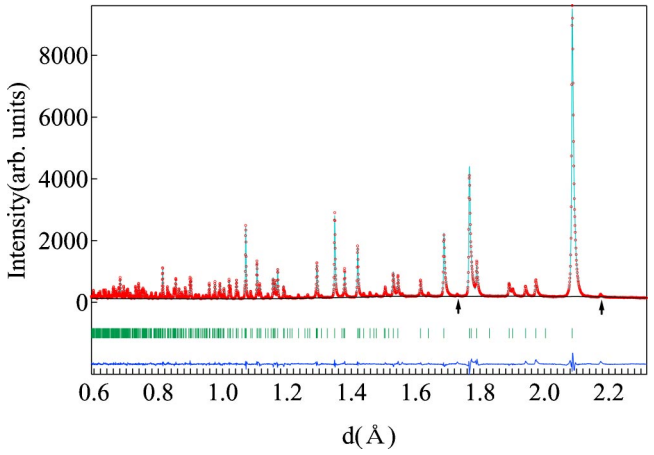

FIG. 2. (Color online) Neutron-diffraction data (symbols) taken at 10 K for $YMnO_3$. The solid line represents the results of Rietiveld refinement with the hexagonal ($P6_3cm$) symmetry. The line at bottom shows the difference curve. The bars indicate the positions of nuclear Bragg peaks. Two peaks marked by arrows are the AF Bragg peaks.

refinement were $R_{wp}=6.29\%$ and $R_p=4.89\%$ for the data shown in Fig. 2. Summary of the refinement results are given in Table I for 10 and 300 K data.

The temperature dependence of lattice parameters obtained from the Rietveld refinement is shown in Fig. 3. The a axis (open circles) gradually expands with increasing temperature whereas the c axis (filled circles) shows negative thermal expansion. This negative thermal expansion behavior is reported to persist up to 1000 K.[13] It is believed that the unusual temperature dependence of the c axis is caused by the tilting of MnO_5 polyhedra accompanied by the buckling of the Y planes. However, the unit cell volume displays the usual positive temperature dependence so decreases upon cooling. It is noticeable that at the antiferromagetic transition temperature both the a- and c-axis lattice constants show clear anomalies. Among the nine position parameters for the

TABLE I. Atomic parameters of $YMnO_3$ determined from high-resolution neutron powder diffraction patterns. The crystal symmetry is hexagonal $P6_3cm$ with the following atomic positions: Y(1) and O(3) at $2a$ $(0,0,z)$; Y(2) and O(4) at $4b$ $(1/3,2/3,z)$; Mn at $6c$ $(x, 0, 0)$; O(1) and O(2) at $6c$ $(x,0,z)$.

	10 K	300 K
Y(1)z	0.2773(7)	0.2727(8)
Y(2)z	0.2318(6)	0.2320(7)
Mn x	0.3423(13)	0.3330(17)
O(1)x	0.3007(4)	0.3076(4)
O(1)z	0.1606(7)	0.1625(7)
O(2)x	0.6399(4)	0.6414(4)
O(2)z	0.3339(6)	0.3360(7)
O(3)z	0.4804(8)	0.4754(9)
O(4)z	0.0193(7)	0.0163(8)
R_{wp}	6.29%	4.19%
R_p	4.89%	3.42%

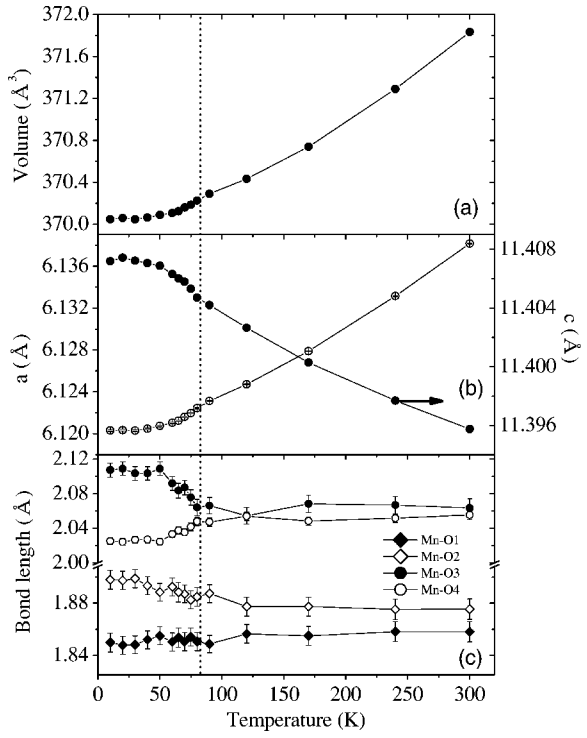

FIG. 3. Temperature variation of (a) unit cell volume, (b) the *a*- and *c*-axis lattice constants, and (c) four Mn–O bond distances. The error bars in (a) and (b) are smaller than the symbol size.

seven atoms listed in Table I, only the *x* and *z* positions of O(1) and O(2) exhibit a sharp decrease, while all five others increase markedly below T_N: for comparison, the temperature dependence seen in the atomic positions of atoms, except for Y(2)*z*, is almost negligible from 300 K to T_N. [Y(2)*z* drops from 0.2320 at 300 K to 0.2297 at 80 K, just above T_N.] These drastic changes seen at T_N in the atomic positions are well represented in the temperature dependence in four Mn–O bond distances as shown in Fig. 3(c). As one can see, there is very weak temperature dependence from 300 K to just above T_N in the four Mn-O distances. However, they all show drastic changes below T_N, although stronger variations are seen for Mn–O(3) and Mn–O(4) bonds. While the Mn–O(4) bond distance decreases below T_N, the Mn–O(3) bond distance increases sharply at the same point. This, then, indicates that, although there is no structural transformation within the resolution of our experiments, spin-lattice coupling is strong enough to produce the different temperature dependences of the Mn–O bond distances on the basal plane: e.g., the Mn–O(3) bond expands upon cooling below T_N, while the Mn–O(4) bond shrinks. It is also to be noted that the Mn–O bond distance [Mn–O(3) and Mn–O(4)] on the basal plane is substantially larger than that for Mn-O(1) and Mn-O(2). It reflects that the topmost occupied Mn *d* orbital is the x^2-y^2 orbital while the *xy* orbital forms a symmetric charge distribution together with the *xz* and *yz* orbitals. The unoccupied $3z^2-r^2$ orbital is 1.7 eV above the degenerate *xy* and x^2-y^2 orbitals.[14] We also note that the bond angle for O(1)–Mn–O(2) is about 180° at room temperature and drops by about 4.5° below T_N while the in-plane bond angle O(3)–Mn–O(4) decreases by about 1.4° from 120°.

Since we have all the information about the atomic positions from 300 to 10 K with very high accuracy, we can study how electric charge distribution, i.e., electric dipole moments, evolves as a function of temperature. For want of the actual value of valence for each atom, we assigned nominal charge values for Y (3+), Mn (3+), and O (2−) for our calculations. Although we acknowledge that this assumption of nominal charge assignment may be oversimplified, nevertheless we believe that our calculation captures the essential temperature variations of the charge distribution inside the unit cell. The use of more realistic charge values would alter our results only quantitatively. After ensuring that we satisfied the charge neutrality inside the unit cell, then we calculated the dipole moments based on the aforementioned model. According to our calculations, the *x* and *y* components of electric dipole moment are zero, independent of temperature. It is because the symmetry ($P6_3cm$) of $YMnO_3$ cancels out the *x* and *y* components of the electric dipole moment. The only nonvanishing component is the *z*-axis component. In our calculations,[15] the dipole moment pointing along the positive *c*-axis direction decreases only slightly from about 41 $\mu C/cm^2$ at 300 with cooling down to 100 K, and shows a significant increase below T_N, indicative of a strong coupling between the electric and magnetic dipole moments. Considering the fact that we have started with a very simple ionic model for the calculations, the electric dipole moment we obtained at 300 K compares well with the reported bulk value of 5.5 $\mu C/cm^2$ at room temperature.[16] In order to show this temperature dependence in a more sensible way independent of the origin we chose in the calculations, we repeated the same calculations with respect to the value at 300 K using the following equation:

$$\Delta\vec{P}(T) = \sum_i q_i(\vec{r_i}(T) - \vec{r_i}(300\ \mathrm{K})), \qquad (1)$$

where q_i, $\vec{r_i}(T)$, and $\vec{r_i}(300\ \mathrm{K})$ are the nominal charge values of each atom and the atomic positions at a given temperature (T) and 300 K in the unit cell, and the sum runs over all atoms inside the unit cell. We present our calculated electric dipole moment ΔP_z (filled circles) in Fig. 4 after normalizing them with respect to the value obtained at 10 K. What is surprising in this temperature dependence of the calculated electric dipole moment is that they follow the almost same temperature dependence as the magnetic moment (open diamonds) taken from our previous neutron diffraction studies.[7] We note that this temperature dependence of ΔP_z is always found regardless of how we choose the unit cell in our calculations. A further interesting point is that when we plot the difference between the Mn–O(3) and Mn–O(4) bond distances they also follow more or less the same temperature dependence as the magnetic moment. The striking observations stress unambiguously that the electric dipole moment is coupled to the magnetic moment through the lattice, i.e., the direct evidence of the coupling between the two order parameters.

Our observation of simultaneous condensation of three order parameters, spin (S), lattice (L) displacement, and electric dipole (D) moment, raises an intriguing question about

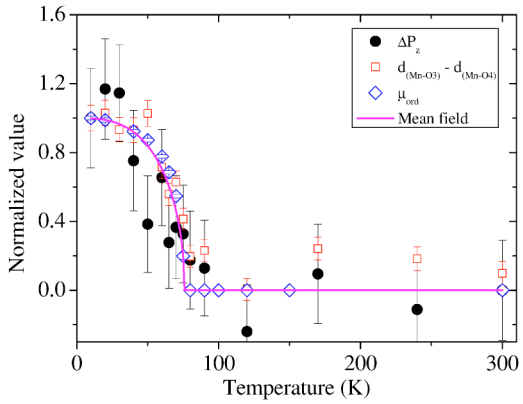

FIG. 4. (Color online) Temperature dependence of ΔP_Z (filled circles), $\Delta d_{\text{Mn-O}}$ (open squares), and μ_{ord} (open diamonds). ΔP_Z is the change in the calculated electric dipole moment with respect to that at 300 K, while $\Delta d_{\text{Mn-O}}$ is a difference between the Mn–O(3) and Mn–O(4) bond distances and μ_{ord} magnetic moments obtained from Ref. 7. The line is for the expected temperature dependence of a mean-field-type order parameter.

the nature of interplay among them. For instance, a Ginzburg-Landau (GL) theory for the coupling between S and L will have a term $-\alpha S^2L^2$. Lower-order coupling is forbidden because of the time-reversal symmetry. On the other hand, a linear coupling between L and D is allowed, $\sim -LD$, in GL theory. As a consequence, L and D condense at the same temperature, T_L, which is lower than T_S for the spin. For a strong spin-lattice interaction strength α, however, the two transition temperatures merge, consistent with the observation. The coupling of S to D, and of D to L, leads to a similar conclusion. On the other hand, we find that the two-dimensional nature of both S and L, in contrast to D, which develops in the z direction, and the fact that displacement of Mn site is likely to lead naturally to displacement of other atoms such as Y, make it plausible that the first scenario (S to L, L to D) is realized in $YMnO_3$. In a different scenario where both L and D couple to S but not to each other, three separate transition temperatures arise, which is difficult to reconcile with the data without a great deal of parameter tuning.

To summarize, we studied the structure of the hexagonal $YMnO_3$ through high resolution neutron diffraction experiments. According to the studies, all structural parameters abruptly change at T_N, which is strong and direct evidence of a spin-lattice coupling. Through this spin-lattice coupling, the electric dipole moment is coupled to the magnetic moment.

We acknowledge W. Jo for providing the powder sample and J. Yu for useful discussion. Work at SungKyunKwan University was supported by the Proton Accelerator User Program (Grant No. M102KS010001-02K1901-01810) and the Center for Strongly Correlated Materials Research.

*Author to whom correspondence should addressed. Electronic address: jgpark@skku.edu

[1] T. Kimura, T. Goto, H. Shintani, K. Ishizaka, T. Arima, and Y. Tokura, Nature (London) **426**, 55 (2003); N. Hur, S. Park, P. A. Sharma, J. S. Ahn, S. Guha, and S.-W. Cheong, *ibid.* **429**, 392 (2004).

[2] M. A. Gilleo, Acta Crystallogr. **10**, 161 (1957).

[3] S. Jin, T. H. Tiefel, M. McCormack, R. A. Fastnacht, R. Mamesh, and L. H. Chen, Science **264**, 413 (1994).

[4] H. Yakel, W. C. Koehler, E. F. Bertaut, and F. Forrat, Acta Crystallogr. **16**, 957 (1963).

[5] Bas B. Van Aken, Thomas T. M. Palstra, Alessio Filippetti, and Nicola A. Spaldin, Nat. Mater. **3**, 164 (2004).

[6] A. Muñoz, J. A. Alonso, M. J. Martinez-Lope, M. T. Casais, J. L. Martinez, and M. T. Fernandez-Diaz, Phys. Rev. B **62**, 9498 (2000).

[7] Junghwan Park, Unggul Kong, A. Pirogov, S. I. Choi, J.-G. Park, Y. N. Choi, Changhee Lee, and W. Jo, Appl. Phys. A: Mater. Sci. Process. **74**, S796 (2002).

[8] T. J. Sato, S.-H. Lee, T. Katsufuji, M. Masaki, S. Park, J. R. D. Copley, and H. Takagi, Phys. Rev. B **68**, 014432 (2003).

[9] Junghwan Park, J.-G. Park, Gun Sang Jeon, Han-Yong Choi, Changhee Lee, W. Jo, R. Bewley, K. A. McEwen, and T. G. Perring, Phys. Rev. B **68**, 104426 (2003).

[10] Z. J. Huang, Y. Cao, Y. Y. Sun, Y. Y. Xue, and C. W. Chu, Phys. Rev. B **56**, 2623 (1997); I. E. Chupis, Low Temp. Phys. **24**, 606 (1998).

[11] M. Fiebig, Th. Lottermoser, D. Fröhlich, A. V. Goltsev, and R. V. Pisarev, Nature (London) **419**, 818 (2002).

[12] T. Ohta, F. Izumi, K. Oikawa, and T. Kamiyama, Physica B **234–236**, 1093 (1997).

[13] T. Katsufuji, S. Mori, M. Masaki, Y. Moritomo, N. Yamamoto, and H. Takagi, Phys. Rev. B **64**, 104419 (2001).

[14] A. B. Souchkov, J. R. Simpson, M. Quijada, H. Ishibashi, N. Hur, J. S. Ahn, S. W. Cheong, A. J. Millis, and H. D. Drew, Phys. Rev. Lett. **91**, 027203 (2003). The on-site *d-d* transition is seen at 1.7 eV for $LuMnO_3$ with the same $P6_3cm$ structure.

[15] As there is ambiguity about how to define the unit cell in calculating the dipole moment for infinite systems like ours, we have chosen for our calculations a unit cell sandwiched between two Y layers keeping the same c axis and the number of atoms inside the cell the same.

[16] Norifumi Fujimura, Tadashi Ishida, Takeshi Yoshimura, and Taichiro Ito, Appl. Phys. Lett. **69**, 1011 (1996); Takeshi Yoshimura, Norifumi Fujimura, Nobuaki Aoki, Kouzo Hokayama, Shigeki Tsukui, Keisuke Kawabata, and Taichiro Itos, J. Korean Phys. Soc. **32**, S1632 (1998).